Internal stresses and resistivity of low-voltage sputtered tungsten films

R.C. Sun, T.C. Tisone, and P.D. Cruzan

Bell Telephone Laboratories, Allentown, Pennsylvania 18103

(Received 24 August 1972)

The continuing development of microelectronic circuits toward greater complexity has stimulated interest in new materials and processes compatible with the currently known silicon device technology. Tungsten has been considered as the first-level conductor for a multilevel structure due to its relatively low electrical resistivity, its thermal expansion coefficient which matches fairly well to that of silicon, its demonstrated good adherence to the dielectrics of interest, and its ability to withstand high-temperature processing. The present work is a part of a study of the dependence of the properties of low-voltage triode sputtered tungsten films upon deposition parameters. The effects on internal stress and resistivity of tungsten films are reported here. Tungsten films have been deposited with thicknesses from 1000 to 15 000 Å and with resistivities as low as 8 $\mu\Omega$ cm (1.55 of the bulk). These films were deposited at 1 μ argon pressure at rates in the range of 50–400 Å/min. The electrical resistivity was observed to increase with increasing deposition rate, decreasing film thickness, and decreasing substrate temperature. The impurity concentration was found to be small by electron microprobe and ion probe techniques and, hence, did not completely account for the observed changes in resistivity. The internal stress was determined by two x-ray methods: (i) precision lattice parameter determination and (ii) a two-exposure technique. In general, depending upon the deposition conditions, tensile or compressive stresses of the order 10^9–10^{10} dyn/cm^2 were observed. The compressive stress was observed to increase with decreasing film thickness and increasing deposition rate. Increasing the substrate temperature caused the compressive stress to decrease to zero and become tensile. This changeover temperature was observed to be 650 °C for a 5000-Å film deposited at 115 Å/min. The observed results are discussed briefly in terms of microstructure changes.

I. INTRODUCTION

The continuing development of microelectronic circuits toward greater complexity has stimulated interest in new materials and processes compatible with the currently known silicon device technology. Initial studies have been devoted to refractory metals for a variety of applications. For instance, tungsten has been considered as the first-level conductor for a multilevel structure due to its relatively low electrical resistivity (5.5 $\mu\Omega$ cm), its thermal expansion coefficient (4.2×10^{-6} °C) which matches fairly well to that of silicon (2.4×10^{-6} °C), its adherence to the dielectrics of interest, and its ability to withstand high-temperature processing. Consequently, there is considerable interest in processes for depositing tungsten films of controlled properties and uniform thickness over typical substrate areas, 18 cm^2.

The present work is a part of a study of the properties of low-voltage sputtered tungsten films as a function of deposition parameters such as film thickness, substrate temperature, and deposition rate. The effects on internal stress and resistivity of tungsten films are reported here. These effects are discussed in terms of film structure and purity.

II. EXPERIMENTAL

A. Film deposition

Substrates used were (100) silicon wafers having about 5000 Å of thermally grown SiO_2. The vacuum system used for film deposition consists of a 6-in. oil diffusion pump with a liquid N_2 cold trap. The plasma discharge is maintained by using a thermionic cathode and is confined in a water-cooled aluminum tube to achieve high ion current with a low argon background pressure. The auxiliary anode voltage is +90 V with respect to ground and the anode current is approximately 6 A. A pressure of less than 5×10^{-7} Torr was reached in the triode sputtering system before the argon gas (99.99% purity) was bled in. Tungsten films were deposited at an Ar pressure of about 1 μ. Substrates were backsputtered at 200 V peak-to-peak for 1 min prior to deposition. Substrate temperature measurements indicate that the steady-state temperature during sputtering at 200 V is 370 °C and that this temperature increases only slightly with increasing cathode voltage (~50 °C at 1000 V). The power density to the substrate due to exposure to the Ar plasma only gives an initial temperature rise of ~3 °C/sec; the initial temperature rise during sputtering at 200 V is ~3.2 °C/sec. The substrate temperature rises to 300 °C within the first two minutes of sputtering and the steady-state temperature is reached within about 10 min after the start of sputtering.

For depositions at elevated temperature the substrates were heated 10 min prior to beginning sputtering. The deposition temperature is defined as that measured immediately after deposition of a 5000-Å tungsten film.

B. Stress determination

The internal stress in tungsten films was determined by two x-ray techniques: (i) precision lattice parameter[1] measurements and (ii) two-exposure techniques.[2] For precise lattice parameter determination, each diffraction peak was scanned at 0.2°/min to locate the approximate position of the peak. From this scan, three points spaced at equal intervals were selected for accurate intensity counting. The peak position, within ±0.01°, was then determined by fitting a parabola to these three data points.[3] It is desirable that these three points have intensities at least 85% of the maximum intensity and straddle the peak of the diffraction line.[4] The lattice parameter was then obtained from a $\cos\theta \cot\theta$ extrapolation which is frequently used to correct for systematic errors.[5] The internal stress S can then be computed from the relation

$$S = \frac{E}{2\nu} \frac{a_0 - a}{a_0}, \tag{1}$$

where a_0 and a are the measured lattice parameters of the standard and the film, respectively, ν is the Pois-

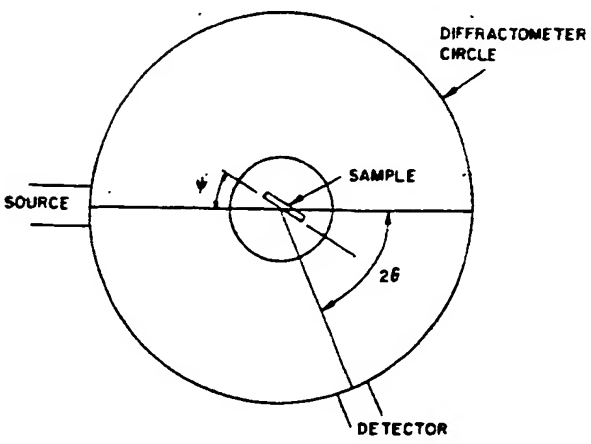

FIG. 1. Schematic of x-ray diffractometer showing ψ rotation. This is a rotation of the sample independent of detector location.

son's ratio, and E is the average Young's modulus of tungsten. In Eq. (1) a biaxial state of stress was assumed to be present in the plane of the film and the two principal stresses are assumed to be equal. The tungsten standard used in this study was a compacted powder (100 mesh) which had been annealed in vacuum for 24 h at 900 °C. In the calculation, values of 0.34 and 34.5 $\times 10^{11}$ dyn/cm^2 were used for ν and E, respectively. The measurements of stress were made from at least two samples for each deposition condition.

For the two-exposure method, the interplanar distance d is determined at two angular orientations ψ to the surface direction in which it is desired to measure the stress. The procedure is to determine the d spacing parallel to the surface $\psi=0$, and again at some chosen value of ψ, typically $\psi=45°$ or 60°, oblique to this direction. A schematic of the diffractometer arrangement showing the ψ rotation is depicted in Fig. 1. The d values are then related to the stress by the following expression[2]

$$S=\frac{d_\psi-d_0}{d_0}\frac{E}{1+\nu}\frac{1}{\sin^2\psi}, \tag{2}$$

where d_ψ is the interplanar spacing at an angle ψ with respect to the sample surface and d_0 is the interplanar spacing parallel to sample surface ($\psi=0°$). The advantage of this technique is that the macroscopic true stress is measured.[6] The microscopic stress caused by stacking fault and solid solutioning, etc., is assumed to be independent of ψ and thus is canceled when two exposures are made.

The (321) peak of tungsten occurring at about 131° was found to be sharp enough for this measurement. Measured intensities were corrected for polarization and Lorentz factors.[4] The peak position was determined by parabola fitting as described above. The sample was then rotated so that $\psi=45°$ and the peak position was determined again. In this case, in addition to the Lorentz and polarization factors, the measured intensity was corrected for the change in absorption factor. This is necessary because the absorption is independent of angle θ at $\psi=0$ but becomes a function of the diffraction angle θ when $\psi\neq 0$.[4]

C. Resistivity

Sheet resistances of the deposited films were determined from four point probe measurements. For thickness measurements, a portion of the film was masked with photoresist and etched to produce a step. The film thickness was then measured across this step using a Zeiss interferometer. The precision of the thickness measurements was approximately 300 Å.

D. Microstructural examination

Transmission electron microscopy (TEM) was used for direct observation of microstructure changes as a function of deposition parameters. The films were prepared by thinning from the back side of the silicon substrate using an ion milling machine. The average grain diameter in the tungsten films was estimated from dark-field and bright-field micrographs by measuring the average diameter of a number of grains (60–70 grains per sample). In cases where the grains were smaller than the transmitted film thickness or not clearly resolved due to the high dislocation density, dark-field techniques were used to obtain images of individual grains, otherwise bright-field images were used. In all cases the dislocation density was too high to resolve individual dislocations even for film thicknesses of the order of 100–200 Å. This would indicate a lower limit of dislocation density in the range of 10^{10}–10^{11} lines/cm^2 within the individual grains.

E. Chemical analysis

Films deposited using the low-voltage system were analyzed for impurity content using electron microprobe and ion microprobe.

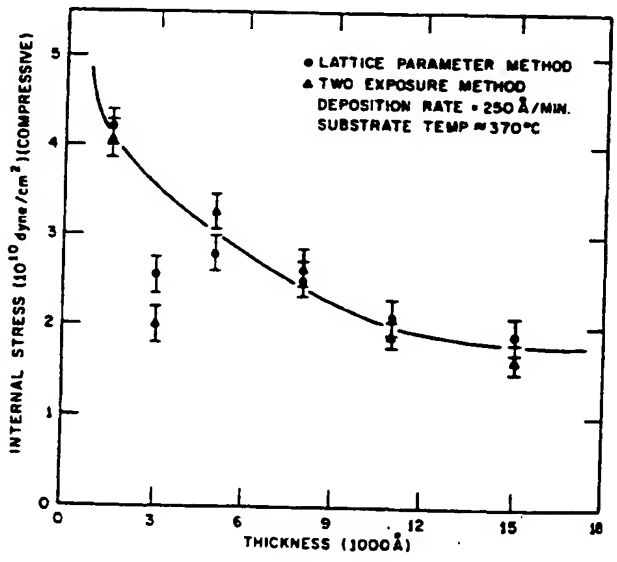

FIG. 2. Internal stresses as a function of tungsten film thickness.

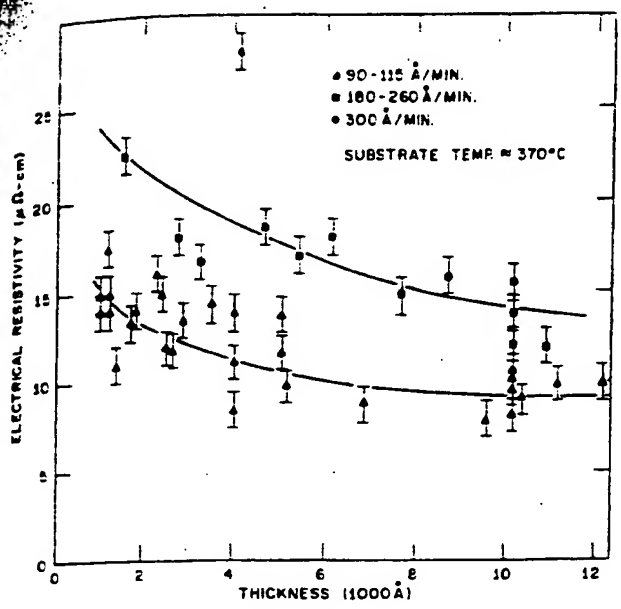

FIG. 3. (a) Electrical resistivity as a function of tungsten film thickness for different deposition rates. (b) Estimated grain size as a function of tungsten film thickness.

III. RESULTS AND DISCUSSIONS

A. Thickness dependence

1. Internal stress

Tungsten films with thicknesses from 1000 to 15 000 Å were deposited by the low-voltage triode sputtering technique at a substrate temperature of 370 °C. The measured internal stress as a function of film thickness is shown in Fig. 2. In this figure, results obtained from both precise lattice parameter measurements and two-exposure methods are represented. It is shown that compressive stresses were observed for all thicknesses. The stress decreases with increasing film thickness. Furthermore, stresses calculated from both methods are in reasonably good agreement within the experimental scatter. Since the true internal stress (that stress not affected by impurities and faulting) is measured by the two-exposure method, it is believed that impurities did not have any significant effects on the observed stress level. This is in agreement with the low impurity concentration illustrated in Table I. Thus only the precise lattice parameter measurements were used for the other studies described in this paper.

There are a number of possible mechanisms which could lead to a decrease in internal stress with increasing thickness. First, the stress in tungsten films could be relieved, as the film grows, by either microstructural rearrangement, or plastic deformation of the underlying dielectric film, or possibly the generation of dislocations in the silicon substrate. Second, since argon entrapment should result in compressive stress in tungsten films, decreasing argon entrapment as the film grows may also be possible. The substrate temperature rise during film growth could result in the annealing out of entrapped argon and lead to lower argon content. However, this seems unlikely for three reasons: (i) The result that the "true" internal stress calculated by the two-exposure method is in good agreement with the result by lattice parameter measurement for all thicknesses indicates that impurities such as argon are in-

TABLE I. Impurity analysis of tungsten films deposited by low-voltage sputtering.

Element	Ion microprobe[a] at.%	Electron microprobe at.%
H	b	
B	...	
C	0.422	1.07—1.23[c,d]
N	1.625	
O	b	1.23—1.90[c,d]
F	...	
Na	0.001	
Mg	0.231	
Al	0.439	
P	0.009	
S	...	
Cl	...	
A		0.01—0.11[c]
K	0.0006	
Ca	0.001	
Cr	0.001	
Fe	0.002	
Ni	0.0002	
Cu	0.004	
Zn	0.001	
Mo	0.020	

[a]These measurements were made by Applied Research Laboratories with the data analysis made using a Carisma Data Reduction Program.
[b]Oxygen and hydrogen were detected but not included in the data reduction.
[c]The indicated ranges of concentration were observed for films deposited with substrate temperature between 350 and 860 °C and voltage between 200 and 1000 V.
[d]A large mean deviation was observed, suggesting that surface contamination of carbon and oxygen was present.

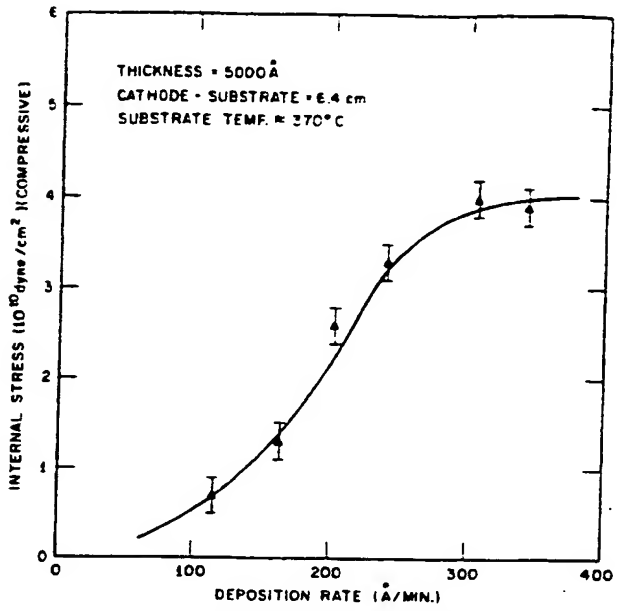

FIG. 4. Internal stress as a function of deposition rate.

significant. (ii) The average Ar concentration is <0.1 at.% and independent of film thickness and deposition temperature; hence it would be difficult to account for the observed stresses and stress gradients with such small concentrations. (iii) Furthermore, Lee and Oblas[7] have shown that argon entrapment is independent of thickness above a critical thickness of about 1000 Å. Consequently, it is unlikely that this mechanism is responsible.

2. Resistivity

The electrical resistivity of thin films is generally higher than the bulk value. The excessive resistivity may be ascribed to the scattering of electrons by structural defects and impurities frozen in during deposition of thin films. The most abundant of these defects are dislocations, typically 10^{10} to 10^{13} lines/cm^2. For low dislocation densities, of the order of 10^8–10^9 lines/cm^2, the dislocation resistivity for tungsten has been reported to be 6.7×10^{-11} $\mu\Omega$ cm^3.[8] For molybdenum[9] and iron[10] values of 5.8×10^{-13} and 1×10^{-12} $\mu\Omega$ cm^3, respectively, have been reported. Also, comparative studies have shown that the dislocation resistivity in tungsten is considerably higher than for niobium, tantalum, and molybdenum.[11] For tungsten it is then expected that dislocations may give a significant contribution to the thin-film resistivity at room temperature for dislocation densities $>10^{10}$ lines/cm^2. Large contributions, of the order 1–6 $\mu\Omega$ cm per at.%[12] to resistivity may arise from vacancies.

Another significant source of electron scattering is the grain boundaries in the film. If the grain size G is of the same order of magnitude as the electron mean free path l scattering at the grain boundaries can increase the resistivity ρ. The observed small values of resistance ratios $[\rho(300\,^\circ\text{K})/\rho(4.2\,^\circ\text{K})]$ for Al[13] and CVD-W[14] films have also previously been interpreted in terms of the effects of grain boundary scattering.

More recently a theoretical treatment of grain boundary scattering superimposed on the scattering from other sources (point defects and phonons) has been put forth.[15] Both the case with surface scattering (Fuchs film thickness effect) and without surface scattering were treated. It was found that surface effects only become significant when $t/l<1$. For bulk tungsten the mean free paths is 413 Å at room temperature.[16] We consider here film thicknesses greater than 1500 Å with resistivities measured at 300 °K so that $t/l>1$ and the Fuchs effect is not important. For the case where only grain boundary effects are important it was found that

$$\rho_0/\rho = 3[\tfrac{1}{3} - \tfrac{1}{2}\alpha + \alpha^2 - \alpha^3 \ln(1+1/\alpha)], \tag{3a}$$

where ρ_0 is the bulk resistivity at very large grain size and ρ is the measured resistivity. The terms α is given by

$$\alpha = \frac{l}{G}\frac{R}{1-R}, \tag{3b}$$

where R is the grain boundary reflection coefficient and is a measure of the strength of the grain boundary scattering. The scattering at the grain boundaries in metals with nonspherical Fermi surfaces contains a strong contribution determined by the orientation differences between the grains and hence R should be large for transition metals like W.[17] Values of R for Al and Cu have been determined to be 0.17 and 0.24, respectively.[17] For finite R and $G \ll l$ then $\rho \propto 1/G$, while for $G \gg l$ then the resistivity is independent of grain size. Such behavior has been observed in Bi thin films where at room temperature l is of the order of microns and a linear relationship was observed between ρ and G for $l \gg G$.[18] For tungsten, with $l = 413$ Å, measurable contributions to the resistivity at room temperature should be observed for $G < 2000$ Å.

Impurities such as argon, hydrogen, oxygen, and nitrogen were concluded to be responsible for the excessive resistivity by a number of workers.[7] The fraction

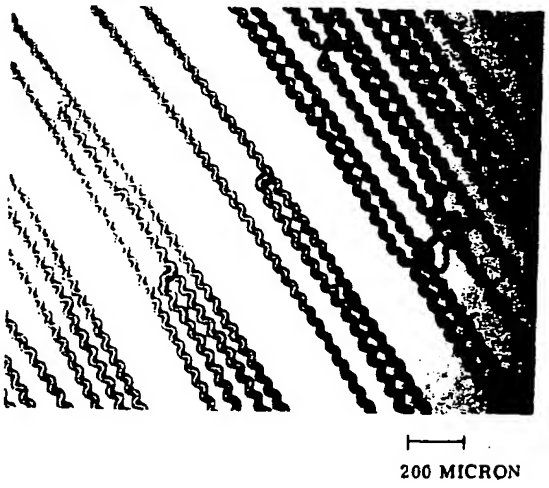

FIG. 5. Optical micrograph of the stress relief patterns of tungsten film deposited at 1000 V (50×).

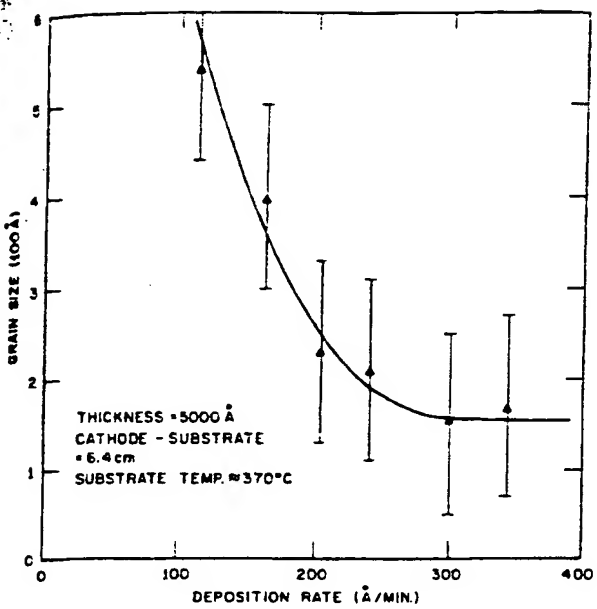

FIG. 6. Calculated grain size as a function of deposition rate.

f_i of impurity of species i trapped in a film can be represented by[17]

$$f_i = \alpha_i N_i/(\alpha_i N_i + P), \tag{4}$$

where N_i is the number of atoms of species i bombarding unit area of film in unit time during deposition, α_i is the effective sticking coefficient of the species i during deposition, and P is the deposition rate of the film. It is clear, that decreasing $\alpha_i N_i$ or increasing P will decrease the fraction of entrapped impurity, and hence there are two ways of decreasing the electrical resistivity. Also, by knowing the dependence of resistivity on some deposition parameters, the mechanism responsible for such resistivity increases can be determined.

The results for the major impurities determined by electron microprobe and ion microprobe techniques are tabulated in Table I. It is to be noted that a number of assumptions about sputtering yields, ionization yields, etc., were made in the data reduction of the ion microprobe analysis. Thus, these impurity concentrations should be considered only estimates, particularly in the case of gaseous impurities like N. Another sensitive indication of N and/or H concentration in the sputtering system is the high sensitivity of the resistivity of Ta films to these impurities (5.1 $\mu\Omega$ cm[18] and 0.8 $\mu\Omega$ cm[19] per at.% solute for N and H, respectively). Using the same deposition technique and conditions, Ta films have been deposited with resistivities as low as 15 $\mu\Omega$ cm (bulk resistivity is 13.7 $\mu\Omega$ cm). The concentrations of N and H estimated from the above result would be less than 0.2 and 2.0 at.%, respectively, assuming either N or H is solely responsible for the increase in resistivity. These results indicate that the impurity content in the films is small and hence is probably not a major contributing factor to the observed stresses and resistivities. The N concentration determined by the ion microprobe (Table I) appears to be an overestimate.

The dependence of electrical resistivity on film thickness for different deposition rates is illustrated in Fig. 3(a). The resistivity of tungsten films deposited at a rate of 90–115 Å/min decreases from about 15 $\mu\Omega$ cm at 1000 Å to 9 $\mu\Omega$ cm at 12 000 Å. It is to be noted that a resistivity of 9 $\mu\Omega$ cm is approximately 60% higher than the bulk value of 5.5 $\mu\Omega$ cm. Furthermore, it is shown that, for all thicknesses, higher resistivity was observed for films prepared at higher deposition rates. The dependence of resistivity on deposition rate will be further discussed in Sec. III B. The scatter of the data, particularly at small thickness, is believed to be due in part to experimental uncertainties in measurements of sheet resistance and film thickness.

The dependence of W grain size on film thickness, as determined by TEM, is shown in Fig. 3(b). This grain size is seen to increase with increasing film thickness. For a film of a given thickness deposited at ambient temperatures (~370 °C), it was noted that the grain size in the vicinity of the tungsten-dielectric interfacial region was much smaller than near the top surface. Near the interface the grain size was ≈100–300 Å while near the outer surface for a 5000-Å film the grain size was 1500–2000 Å. There is thus a gradient in grain size and possibly dislocation density across the film thickness.

It has been suggested that both the small grain size and high dislocation density can give rise to measurable contribution to the room-temperature resistivity of W. Figures 3(a) and 3(b) show a decrease in resistivity and an increase in grain size with an increase in film thickness. It thus appears that the decrease in resistivity may be associated with the increase in grain size. This is supported by the fact that the measured grain sizes are of the same order of magnitude expected to

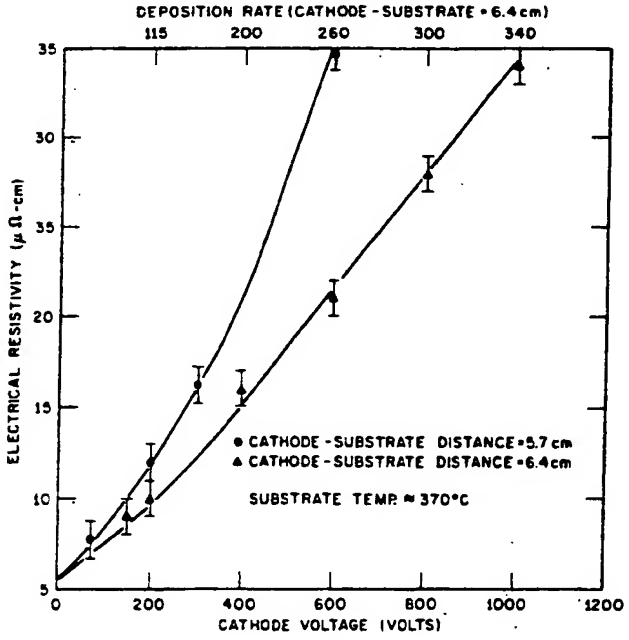

FIG. 7 Electrical resistivity as a function of cathode voltage for two different cathode-to-substrate distances.

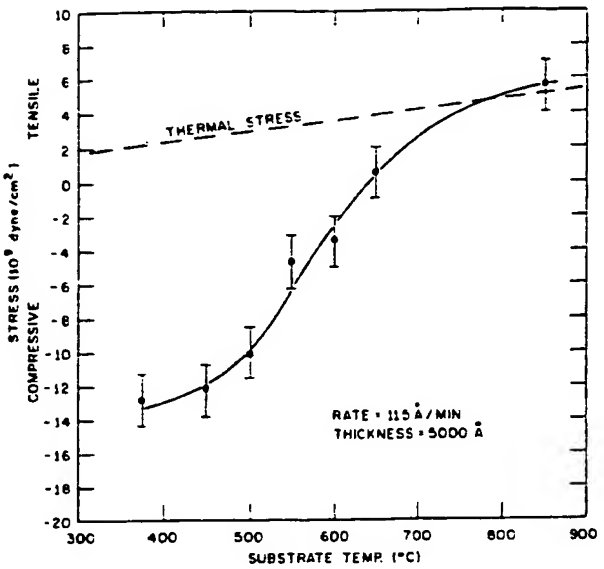

FIG. 8. Internal stress as a function of substrate temperature during deposition.

give an appreciable contribution to the resistivity through grain boundary scattering.

B. Deposition rate dependence

1. Internal stress

The deposition rate is a function of several experimental parameters including cathode voltage, cathode current, cathode-substrate distance, argon pressure, discharge current, and substrate bias voltage. In this investigation, cathode voltage was chosen as the only rate-determining variable for internal stress measurement. Figure 4 shows the result that the stress increases from 7×10^9 dyn/cm² at a deposition rate of 115 Å min to 4×10^{10} dyn/cm² at a rate of 330 Å/min.

The incidence of adhesion failures for 5000-Å-thick film deposition at 370 °C increased with increasing cathode voltage. For 600-V (260 Å/min) and higher the adhesion was poor. Apparently, for voltages of 600 V and greater, the resulting compressive stress (~4×10^{10} dyn/cm²) in the film is too great to be supported by the adhesive bond between the film and the substrate. An example of a buckled film of thickness 10 000 Å resulting from a deposition rate of 300 Å/min, at 370 °C is shown in Fig. 5. The films deposited at these higher rates were buckled when the wafers were removed from the station or shortly thereafter. Large numbers of parallel sinusoidal waves with wavelength of about 50 μ are ridges of tungsten films buckled from the substrate. Occasionally these buckled waves split into many individual sinusoidal waves. The buckled waves seem to occur initially and more closely on the side of the slice where the film is thicker and follow the thickness contours toward the thinner side. This is probably because the shear stress at the film-substrate interface increases with increasing film thickness, until the adhesion of the film to the substrate is not sufficient to prevent separation from the substrate.

The x-ray line broadening was observed to increase with increasing deposition rates. Generally this broadening is caused by small grain size and inhomogeneous strain. Assuming that the observed line broadening is due to small grain size, the change of grain size as a function of deposition rate can be estimated by[20]

$$G = 0.9\lambda/\beta\cos\theta, \tag{5}$$

where G, λ, β, and θ denote grain size, wavelength of the Cu K_α (1.542 Å) radiation, corrected half-width of the peak, and the Bragg angle, respectively. The half-width of the (110) peak having a Bragg angle of 40° was used for the calculation. Figure 6 illustrates the estimated grain size as a function of deposition rate. It is shown that the grain size decreases from 540 to 150 Å as the deposition rate increases from 115 to 336 Å/min. Furthermore, the decrease is more rapid from 115 to 200 Å/min and levels off at about 180 Å for higher reposition rates.

2. Electrical resistivity

The electrical resistivity of low-voltage sputtered tungsten films was observed to increase with increasing cathode voltage and decreasing cathode-to-substrate distance. Figure 7 illustrates the case for cathode-to-substrate separations of 5.7 and 6.4 cm, respectively. Such observations suggest that the resistivity change is primarily due to microstructural changes, rather than impurities, since the relationship between deposition rate and impurity content [Eq. (4)] predicts the reverse trend for impurities. However, a good correlation is found between the decrease in grain size and corresponding increase in resistivity with increasing deposition rate (see Fig. 6). The grain sizes (Fig. 6) in the range of 100–500 Å are in the region of the bulk mean free path of 413 Å and resistivities (Fig. 7) of up to 5 times bulk were observed. This further supports the

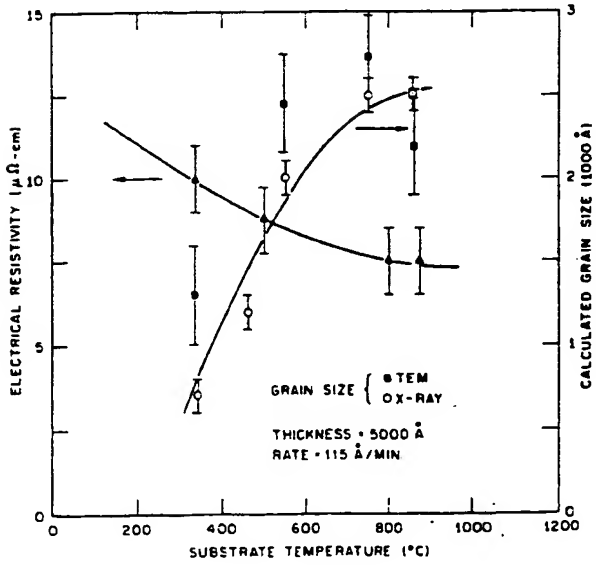

FIG. 9. Electrical resistivity as a function of substrate temperature during deposition.

argument that the observed changes in resistivity are predominately due to the decrease in grain size and possible increase in dislocation density with increasing deposition rate.

C. Substrate temperature dependence

1. Internal stress

The dependence of internal stress on the substrate temperature was investigated in order to obtain tungsten films with minimal stresses. Figure 8 shows the results which indicate that the internal stresses changed from compression to tension at about 650 °C for a film thickness of 5000 Å. Further increases in substrate temperature resulted in higher tensile stresses. Similar results were reported in bias-sputtered molybdenum films.[21] This result can be used advantageously to produce stress-free tungsten films by depositing at a temperature of 650 °C. Furthermore, as will be described later, resistivity can also be reduced by depositing at elevated substrate temperatures.

The observed increase in tensile stress with increasing substrate temperature is expected to be influenced by an increasing thermal stress contribution. The thermal stress, S_T, can be expressed by the equation

$$S_T=(\alpha_F-\alpha_S)\Delta T E, \tag{6}$$

where α_F and α_S are the coefficients of thermal expansion for the tungsten film (4.2×10^{-6} cm/°C) and silicon substrates (2.4×10^{-6} cm/°C)[22], respectively, at room temperature, ΔT is the temperature of the substrate at the completion of film deposition minus the temperature at which the stress is measured, and E is the Young's modulus of tungsten. Accordingly, the tensile stress component in a tungsten film would increase as the substrate temperature increases. The calculated thermal stress is indicated by the dashed line on Fig. 8 for comparison. This thermal stress is probably an upper estimate since the thermal expansion coefficient of Si increases with temperature.[23] It is evident that the magnitude of the change in thermal stress with substrate temperature is too small to account for the observed change of the measured stress in W. Consequently, it is suspected that the predominant component of the internal stress in W film is a function of the detailed microstructure of the film, which in turn is a function of the substrate temperature during deposition.

TEM observations showed that the grain size in the region of the metal-dielectric interface increased with increasing deposition temperature, and, at the same time, the grain size gradient across the film thickness decreased. The average grain size as determined from both x-ray and TEM measurements is shown in Fig. 9. It is also seen in this figure that the average grain size also increases with increasing deposition temperature.

2. Electrical resistivity

The electrical resistivity of tungsten films was observed to decrease with increasing substrate temperature as shown in Fig. 9. Such a decrease is believed to be due to microstructure changes. The grain sizes estimated from x-ray and transmission measurements are also shown in Fig. 9. The grain size increases from 700 Å to about 2500 Å as the substrate temperature increases from 350 °C to 860 °C. Again there is a good correlation between the decrease in resistivity and increase in grain size.

D. Evaluation of grain boundary resistivity

The experimental results presented here suggest that the grain size is the dominant factor in determining the film resistivity. From the structural observations of film grain size we can then estimate the grain boundary reflection coefficient R for tungsten films using Eqs. (3a) and (3b). From the data in Figs. 3 and 9, where the grain size was measured directly, R was calculated to be ~0.65. Using the data from Figs. 6 and 7, where the grain size was estimated from x-ray measurements, R ~0.5. In general the grain size estimated by x-ray was smaller than the observed TEM grain size as shown in Fig. 9.

The estimated value of R (0.5—0.65) for tungsten is much larger than observed for Al and Cu with values of 0.18 and 0.24, respectively. This is consistent with the more complicated Fermi surface of tungsten[16] as compared to Cu and Al which is expected to give rise to a stronger grain boundary scattering.

IV. SUMMARY

The internal stresses and electrical resistivity of low-voltage sputtered tungsten films have been investigated as a function of film thickness, deposition rate, and substrate temperature. The internal stress was determined to be compressive and was observed to decrease with increasing film thickness and decreasing deposition rate for films deposited below 650 °C. With increasing substrate temperatures, the stress changes to tensile. Deposition temperatures of about 650 °C result in films with no measurable stress for 5000-Å films deposited at a rate of 115 Å/min. The electrical resistivity of tungsten films was observed to decrease with increasing film thickness, decreasing deposition rate, and increasing substrate temperature. These observations were attributed to microstructural changes, not impurities. From these results, the proper deposition conditions for optimizing internal stress and resistivity can be obtained.

[1] B. D. Cullity, *Elements of X-Ray Diffraction* (Addison-Wesley, Reading, Mass., 1956), p. 436.
[2] F. Gisen, R. Glocker, and E. Osswald, Z. Tech. Phys. 17, 145 (1936).
[3] D. P. Koistinen and R. E. Morburger, Trans. Am. Soc. Met. 51, 537 (1959).
[4] Society of Automotive Engineers Technical Report No. TR-182 (unpublished).
[5] A. Taylor and H. Sinclair, Proc. Phys. Soc. Lond. 57, 126 (1945).
[6] G. A. Walker and C. C. Goldsmith, J. Vac. Sci. Technol. 1, 569 (1970).
[7] W. W. Lee and D. Oblas, Solid State Technol. 7, 129 (1970).
[8] H. B. Shukovsky, R. M. Rose, and J. Wulff, Acta Metall. 14, 821 (1966).
[9] L. D. Whitmire and F. B. Brotzen, Trans. Am. Inst. Min. Eng. 239, 824 (1967).
[10] L. J. Cuddy, Philos. Mag. 12, 855 (1965).
[11] F. Krautz and H. Schultz, Z. Angew. Phys. 15, 1 (1963).

[12]K. L. Chopra, *Thin Film Phenomena* (McGraw-Hill, New York, 1969), p. 381.
[13]A. F. Mayadas, R. Feder, and R. Rosenberg, J. Vac. Sci. Technol. 6, 690 (1969).
[14]A. F. Mayadas, J. J. Cuomo, and R. Rosenberg, J. Electrochem. Soc. 116, 1742 (1969).
[15]A. F. Mayadas and M. Shatzkes, Phys. Rev. B 1, 1382 (1970).
[16]E. Fawcett and D. Griffiths, J. Phys. Chem. Solids 23, 1631 (1962).
[17]L. I. Maissel and R. Glang, *Handbook of Thin Film Technology* (McGraw-Hill, New York, 1970), pp. 4–20.
[18]F. Gebhardt, H. D. Sighezzi, and W. Durrschnobel, Z. Metallkd. 49, 577 (1958).
[19]J. A. Pryde and I. S. T. Tsong, Trans. Faraday Soc. 67, 297 (1971).
[20]H. P. Klug and L. E. Alexander, *X-Ray Diffraction Procedures* (Wiley, New York, 1954), p. 512.
[21]R. Glang, R. A. Holmwood, and P. C. Furois, *Advances in Vacuum Science and Technology*, edited by H. Adams (Pergamon, New York 1965), Vol. 2, Part 3, p. 643.
[22]*Metal Handbook* (American Society of Metals, Metals Park, Ohio, 1948), p. 21.
[23]L. Maissel, J. Appl. Phys. 31, 211 (1960).

Journal of APPLIED PHYSICS

Volume 44 March 1973 Number 3

a publication of the American Institute of Physics

nal of APPLIED PHYSICS

Vol. 44, No. 3, March 1973

(Continued on p. ii)